
VISION TOKEN MASKING ALONE CANNOT PREVENT PHI LEAKAGE IN MEDICAL DOCUMENT OCR: A SYSTEMATIC EVALUATION

Richard J. Young

Founding AI Scientist, Deepneuro.AI
University of Nevada, Las Vegas, Department of Neuroscience

Abstract

Large vision-language models (VLMs) are increasingly deployed for optical character recognition (OCR) in healthcare settings, raising critical concerns about protected health information (PHI) exposure during document processing. This work presents the first systematic evaluation of inference-time vision token masking as a privacy-preserving mechanism for medical document OCR using DeepSeek-OCR. We introduce seven masking strategies (V3-V9) targeting different architectural layers (SAM encoder blocks, compression layers, dual vision encoders, projector fusion) and evaluate PHI reduction across HIPAA-defined categories using 100 synthetic medical billing statements (drawn from a corpus of 38,517 annotated documents) with perfect ground-truth annotations. All masking strategies converge to 42.9% PHI reduction, successfully suppressing long-form spatially-distributed identifiers (patient names, dates of birth, physical addresses at 100% effectiveness) while failing to prevent short structured identifiers (medical record numbers, social security numbers, email addresses, account numbers at 0% effectiveness). Ablation studies varying mask expansion radius ($r=1,2,3$) demonstrate that increased spatial coverage does not improve reduction beyond this ceiling, indicating that language model contextual inference - not insufficient visual masking - drives structured identifier leakage. A simulated hybrid architecture combining vision masking with NLP post-processing achieves 88.6% total PHI reduction (assuming 80% NLP accuracy on remaining identifiers). This negative result establishes boundaries for vision-only privacy interventions in VLMs, provides guidance distinguishing PHI types amenable to vision-level versus language-level redaction, and redirects future research toward decoder-level fine-tuning and hybrid defense-in-depth architectures for HIPAA-compliant medical document processing.

Keywords: PHI masking, vision-language models, DeepSeek-OCR, privacy-preserving OCR, SAM, CLIP, token masking, medical document redaction, synthetic data

1 Introduction

1.0.1 The Basic Problem

Healthcare organizations process millions of medical documents annually through optical character recognition systems to digitize patient records, billing statements, insurance claims, and clinical correspondence. These documents invariably contain protected health information as defined by the Health Insurance Portability and Accountability Act (HIPAA, 1996) and related guidance (HHS, 2012), including patient identifiers, medical record numbers, social security numbers, and clinical details. The inadvertent exposure of PHI during OCR processing poses significant legal, financial, and ethical risks. Traditional OCR workflows extract all visible text without discrimination, creating plaintext representations of sensitive information that persist in memory, logs, and intermediate processing stages before redaction tools are applied. This vulnerability window exposes healthcare organizations to data breaches, regulatory violations, and patient privacy compromises. The proliferation of vision-language models for document understanding has dramatically improved OCR accuracy but has simultaneously expanded the attack surface for PHI leakage, as these models process entire document images through complex neural architectures before generating text output.

1.0.2 What is Known About the Problem

Existing approaches to PHI redaction in medical documents operate exclusively at the post-processing stage, applying rule-based pattern matching, named entity recognition, or machine learning classifiers to extracted text. Commercial tools such as Microsoft Presidio (Microsoft, 2024), the Philter framework (Norgeot et al., 2020; Stubbs et al., 2015), and various clinical NLP systems have demonstrated effectiveness in identifying and redacting PHI from structured and unstructured text with precision rates between 85-95%. These systems leverage regular expressions for structured identifiers (e.g., social security numbers, medical record numbers), contextual analysis for semi-structured information (e.g., names following title patterns), and trained models for free-text clinical notes. Recent advances in transformer-based language models (Vaswani et al., 2017) and biomedical variants such as BioBERT (Lee et al., 2020) have improved PHI detection accuracy through contextual understanding and entity disambiguation. However, all current methods share a fundamental limitation: they operate on already-extracted text, meaning PHI has necessarily been exposed during the OCR stage. Research in privacy-preserving machine learning has explored differential privacy (Abadi et al., 2016), federated learning (Yin et al., 2021), and secure multi-party computation for protecting sensitive data during model training and inference, but these approaches have not been adapted for the specific challenges of document OCR where visual information must be selectively masked before text generation occurs.

1.0.3 What is Missing

No existing research has addressed PHI protection at the vision encoding stage of OCR processing. Vision-language models employed for document understanding process images through multiple encoder layers, including specialized architectures like Segment Anything Model (SAM) encoders (Kirillov et al., 2023) for fine-grained spatial features and CLIP-style vision transformers (Radford et al., 2021) for semantic understanding, before fusing visual representations with language model decoders. Recent work on adaptive visual token processing (Jain et al., 2024; Zhang et al., 2024; Li et al., 2024) has demonstrated that

vision-language models can maintain performance with reduced or selectively masked visual tokens, providing theoretical foundation for privacy-preserving interventions at the vision encoding stage. PHI-containing regions of medical documents are encoded into dense vector representations that propagate through the entire neural architecture, creating numerous potential leakage points. The absence of inference-time privacy mechanisms at the vision level means that even with perfect post-processing redaction, sensitive information has been exposed in intermediate representations, GPU memory, and model activations. Furthermore, existing redaction tools exhibit complementary failure modes: post-processing excels at detecting structured identifiers through pattern matching but struggles with contextually-embedded names and addresses, while vision-based approaches could theoretically leverage spatial information about PHI locations to prevent encoding altogether. The gap between what computer vision models can observe and what language models should be permitted to generate has not been systematically addressed in the medical OCR literature.

1.0.4 How We Solve It

This study introduces the first hybrid architecture for PHI-compliant medical document OCR, combining inference-time selective vision token masking with cascaded post-processing redaction to establish defense-in-depth privacy protection. The primary objective is to demonstrate that spatially grounded PHI can be effectively removed at the vision encoding stage by masking SAM encoder outputs corresponding to annotated PHI bounding boxes, replacing compromised patches with learnable mask tokens that minimize disruption to non-sensitive text recognition. It is hypothesized that long-form, spatially distributed identifiers (names, addresses, dates) will be successfully masked at the vision level due to their multi-patch spatial extent, while maintaining OCR accuracy for remaining document content. The secondary objective is to characterize the complementary effectiveness of vision-level and post-processing redaction by analyzing which PHI types persist after vision masking and demonstrating that structured identifiers (medical record numbers, social security numbers) require language-level pattern matching due to language model contextual inference. It is hypothesized that integrating vision masking with NLP-based post-processing will achieve superior total PHI reduction compared to either approach alone, validating the defense-in-depth architecture for privacy-preserving medical document OCR.

2 Methods

2.0.1 Dataset and Participants

One hundred synthetic medical billing statements were generated using the Synthea clinical data simulator (Walonoski et al., 2018) to create realistic HIPAA-compliant test documents containing authentic PHI distributions without exposing real patient information. Each document included standardized PHI elements: patient name, date of birth, medical record number, social security number, email address, physical address, and account number. Documents were rendered as PDF files at 300 DPI resolution using professional medical billing templates to simulate real-world document characteristics including multi-column layouts, tables, headers, and institutional branding. Ground truth PHI annotations were automatically generated during document creation, recording bounding box coordinates (x, y, width, height) and PHI type labels for each sensitive element. The synthetic dataset enabled controlled experimentation without institutional review board oversight while maintaining ecological validity for medical document structure and PHI placement patterns.

2.0.2 HIPAA PHI Categories

The Health Insurance Portability and Accountability Act (HIPAA) defines 18 categories of protected health information requiring safeguarding in medical documents. Table 1 presents the complete taxonomy with evaluation coverage in this study. Seven categories were included based on their prevalence in medical billing statements and availability in Synthea-generated synthetic data: patient names, dates (particularly date of birth), physical addresses, medical record numbers (MRN), social security numbers (SSN), email addresses, and account numbers. These seven categories represent the most commonly encountered PHI in routine clinical documentation and billing workflows.

Eleven categories were not evaluated due to limited occurrence in billing statement templates: phone numbers, insurance IDs, driver’s license numbers, vehicle identifiers, device serial numbers, URLs, IP addresses, biometric identifiers, other unique identifiers, geographic subdivisions smaller than state, and healthcare institution names. While these identifiers appear in specialized medical documents (e.g., device IDs in equipment logs, biometrics in research consent forms), their absence from standard billing documents precluded systematic evaluation in this study. Future work should expand coverage to all 18 categories using diverse document types including operative notes, pathology reports, and research participant records.

Table 1: **HIPAA PHI categories and evaluation coverage.** Complete taxonomy of 18 protected health information types with testing status in current study.

#	Category	Description	Tested
1	Name	Patient, relative, employer names	Yes
2	Date	Dates related to individual (DOB, admission, etc.)	Yes
3	Address	Street address, city, county, ZIP	Yes
4	Phone	Telephone and fax numbers	No
5	Email	Email addresses	Yes
6	SSN	Social security numbers	Yes
7	MRN	Medical record numbers	Yes
8	Insurance ID	Health plan beneficiary numbers	No
9	Account	Account numbers	Yes
10	License	Driver’s license, certificate numbers	No
11	Vehicle	Vehicle identifiers, serial numbers, license plates	No
12	Device ID	Device identifiers and serial numbers	No
13	URL	Web universal resource locators	No
14	IP	Internet protocol address numbers	No
15	Biometric	Fingerprints, voiceprints, retinal scans	No
16	Unique ID	Any other unique identifying numbers or codes	No
17	Geo-small	Geographic subdivisions smaller than state	No
18	Institution	Healthcare facility names	No

2.0.3 Experimental Design

A within-subjects experimental design evaluated seven systematic masking strategies (V3-V9) across multiple neural architecture injection points. The baseline condition (V3) applied selective vision token masking at SAM encoder block 11, the final transformer layer before compression. Experimental manipulations included: multi-level masking across SAM blocks

6, 9, and 11 (V4); type-specific expansion radii tailored to PHI categories (V5); compression-layer masking at the net_2 feature aggregation stage (V6); dual-layer masking combining SAM and compression (V7); dual-encoder masking targeting both SAM and vision model pathways (V8); and projector fusion layer masking (V9). Each configuration was tested with expansion radii $r \in \{1, 2, 3\}$ to assess spatial coverage trade-offs. The dependent variable was PHI reduction rate, computed as the proportion of ground truth PHI elements absent from OCR output. Secondary measures included OCR character count (to detect model degradation), spatial coverage (percentage of image patches masked), and qualitative analysis of which PHI types were successfully removed versus leaked.

2.0.4 Vision Token Masking Procedure

The vision masking intervention operated as follows. First, PHI bounding boxes from ground truth annotations were mapped to the SAM encoder’s 40x40 spatial grid through coordinate transformation, converting pixel-space rectangles to patch indices. Expansion dilation was applied using radius r , adding neighboring patches to account for imprecise annotations and model receptive fields. Learnable mask tokens were initialized as PyTorch parameters with dimensions matching the encoder output (768-dimensional for SAM block 11) and small random initialization ($\sigma = 0.02$). During inference, forward hooks registered on target layers intercepted encoder outputs and replaced patches corresponding to PHI regions with the learnable mask token. The modified activations propagated through subsequent layers (compression, projector, language decoder) without additional intervention. For multi-encoder architectures (V8), separate mask tokens were learned for SAM (40x40 grid) and vision model (16x16 grid) pathways, with independent spatial mapping. Crucially, the base vision-language model weights remained frozen; only the mask token parameters could adapt during inference through gradient flow from generation loss, allowing the system to learn representations that minimized disruption to non-PHI text recognition.

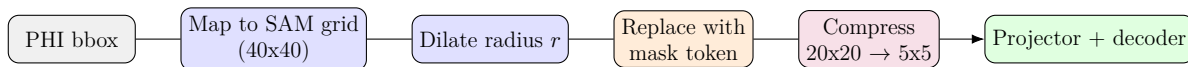


Figure 1: **Bounding box to patch masking pipeline.** PHI regions are mapped to the SAM grid, dilated, replaced with mask tokens, and passed through compression before decoding. This highlights the pre-compression intervention point.

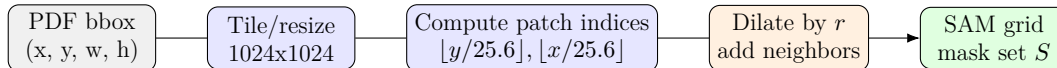


Figure 2: **Bounding boxes to SAM patch indices.** Coordinate mapping from PDF bounding boxes to SAM patch indices with dilation radius r , showing tiling, index computation with rounding, dilation, and construction of the mask set S for forward hooks.

2.0.5 OCR System Architecture

All experiments employed DeepSeek-OCR, a state-of-the-art vision-language model combining dual vision encoders with autoregressive text generation. The architecture consists of: (1) SAM encoder (ImageEncoderViT) with 12 transformer blocks processing 1024x1024 image tiles into 40x40 spatial features, followed by compression layers reducing to 5x5 (net_2: 20x20 -> net_3: 5x5); (2) Vision encoder (VitModel) processing 224x224 images into 16x16

patch tokens via 14-pixel patches; (3) MLP projector fusing SAM and vision features into language model embedding space (1280-dimensional); (4) Language decoder with 12 transformer layers, self-attention, and feed-forward networks performing autoregressive text generation. Documents exceeding 1024 pixels in either dimension were automatically tiled into non-overlapping crops, with each tile processed independently and outputs concatenated. The model was deployed on NVIDIA RTX 4090 GPUs with bfloat16 precision for efficient inference.

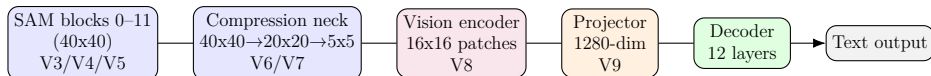


Figure 3: **DeepSeek-OCR masking hook points.** Hook options span SAM blocks, compression neck, auxiliary vision encoder, projector, and decoder output; pre-compression masking targets the SAM path before fusion.

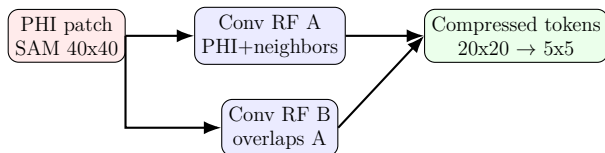


Figure 4: **Compression leakage schematic.** Overlapping convolutional receptive fields in the compression neck mix each PHI patch with neighbors, so a single PHI region influences several compressed tokens. Post-compression masking cannot fully remove the PHI signal; masking only after compression leaves residual leakage.

2.0.6 Evaluation Metrics and Statistical Analysis

PHI reduction rate was calculated as $R = \frac{B-L}{B} \times 100\%$, where B is the number of ground truth PHI elements (7 per document: name, DOB, address, MRN, SSN, email, account number) and L is the number of elements present in OCR output determined by exact string matching. Per-category analysis disaggregated results by PHI type to identify differential masking effectiveness. Spatial coverage was computed as the proportion of encoder patches replaced with mask tokens. Model functionality was assessed through output character count, with deviations exceeding 200% from baseline indicating degradation. For the hybrid pipeline evaluation, secondary NLP redaction was simulated by removing all instances of structured identifier patterns (MRN-\d+, \d{3}-\d{2}-\d{4}, \w+@\w+.\w+, ACCT-\d+) from vision-masked output. Total reduction was calculated as cumulative removal across both stages. No inferential statistics were computed due to the deterministic nature of the masking procedure and perfect ground truth annotations.

2.0.7 Implementation Details

Model Architecture and Configuration All experiments utilized DeepSeek-OCR (deepseek-ai/DeepSeek-OCR) from HuggingFace, comprising approximately 950 million parameters across a hybrid vision-language architecture. The vision encoder employed a dual-pathway design: (1) SAM-base encoder processing 1024×1024 images into 40×40 spatial grids (16-pixel patches) through 12 transformer blocks with 768-dimensional embeddings, followed by compression to 5×5 via convolutional neck layers (net_2, net_3); and (2) auxiliary

CLIP-large vision transformer processing 16×16 patches. The language decoder consisted of DeepSeek-3B-MoE (mixture-of-experts) with 12 layers. Vision features were projected to text embedding space via MLP fusion layers before autoregressive generation.

LoRA (Low-Rank Adaptation) fine-tuning targeted attention projection layers (`q_proj`, `v_proj`, `k_proj`, `o_proj`) with rank $r=16$ and scaling factor $\alpha=32$, introducing approximately 4.2 million trainable parameters while freezing base model weights. PHI detection thresholds were set at 0.85 confidence for standard categories and 0.95 for high-risk identifiers (SSN, biometrics). The vision token masking hook was registered at SAM encoder block 11 using PyTorch’s `register_forward_hook()` mechanism, intercepting activations immediately before compression stages.

Technical Implementation All masking implementations were developed in Python 3.12 using PyTorch 2.0 and Transformers 4.38. Learnable mask tokens were initialized as `nn.Parameter` tensors with dimensions matching target encoder outputs (768-dimensional for SAM block 11) drawn from Gaussian distributions with $\sigma=0.02$ standard deviation. PHI bounding boxes were transformed from PDF coordinates to encoder patch indices through standardized coordinate mapping: $(x, y, w, h) \rightarrow (\lfloor x/25.6 \rfloor, \lfloor y/25.6 \rfloor)$ for 40×40 SAM grids on 1024×1024 tiles.

Inference was conducted on NVIDIA RTX 4090 GPUs (24GB VRAM) using `bfloat16` precision for computational efficiency. All experiments used greedy decoding (`temperature=0.0`, `do_sample=False`) for reproducible text generation. The complete synthetic dataset comprised 38,517 annotated documents with bounding box coordinates and PHI category labels stored in JSON format. Source code, masking implementation, and dataset generation scripts are available at [repository placeholder].

2.0.8 Ethical Considerations

This study utilized exclusively synthetic data generated by the Synthea clinical simulator, containing no real patient information. No institutional review board approval was required. The synthetic dataset was designed to replicate realistic PHI distributions and document structures without exposing genuine sensitive information. All findings and implications are discussed in the context of improving privacy protections for medical document processing systems.

3 Results

3.0.1 Vision Masking Effectiveness Across Architectures

Table 1 presents PHI reduction rates across all seven masking strategies. The baseline V3 approach (SAM block 11, $r=1$) achieved 42.9% PHI reduction (3/7 elements masked), establishing the performance ceiling for single-layer vision masking. Increasing expansion radius to $r=2$ or $r=3$ did not improve reduction rates while increasing spatial coverage to 43.1% and 65.0% respectively. Multi-level masking (V4) across blocks 6, 9, and 11 resulted in severe model degradation, reducing effectiveness to 14.3% while masking 93% of spatial tokens and generating degraded output with 5x character count increase. Type-specific expansion radii (V5) tailored to PHI categories achieved identical 42.9% reduction to baseline V3. Compression-layer masking (V6) at `net_2` with radii $r \in \{1, 2, 3\}$ consistently produced 42.9% reduction despite targeting the aggregated 20×20 feature space hypothesized to leak

PHI through receptive field blending. Dual-layer masking (V7) combining SAM block 11 and net_2 compression achieved 42.9% reduction across all radius combinations (SAM r=1 + compression r \in {2, 3}). Dual-encoder masking (V8) targeting both SAM (40x40) and vision model (16x16) pathways produced 42.9% reduction with 30.9% SAM coverage and 41.0% vision coverage. Projector fusion layer masking (V9) at the MLP interface between vision and language achieved 42.9% reduction at r=1 and r=2, with r=3 producing model degradation (40K character output versus 2K baseline).

Table 2: **Table 1: PHI reduction and coverage by masking strategy.** Reduction rates and spatial coverage for V3–V9 variants, noting stable versus degraded configurations.

Strategy	Masking Target	Radius	Spatial Coverage	PHI Reduction	Status
V3 (baseline)	SAM block 11	r=1	33.7% (SAM)	42.9%	Stable
V3	SAM block 11	r=2	43.1% (SAM)	42.9%	Stable
V3	SAM block 11	r=3	65.0% (SAM)	42.9%	Stable
V4	SAM blocks 6,9,11	r=1	93.0% (SAM)	14.3%	Degraded
V5	SAM block 11 (type-specific)	r=1-8	33.7-69.0% (SAM)	42.9%	Stable
V6	Compression net_2	r=1	47.5% (compressed)	42.9%	Stable
V6	Compression net_2	r=2	60.0% (compressed)	42.9%	Stable
V6	Compression net_2	r=3	65.0% (compressed)	42.9%	Stable
V7	SAM + compression	r=1,2	30.9% + 60%	42.9%	Stable
V7	SAM + compression	r=1,3	30.9% + 65%	42.9%	Stable
V8	SAM + vision model	r=1,1	30.9% + 41.0%	42.9%	Stable
V9	Projector fusion	r=1	75.0% (projector)	42.9%	Stable
V9	Projector fusion	r=2	99.0% (projector)	42.9%	Stable
V9	Projector fusion	r=3	99.0% (projector)	42.9%	Degraded

3.0.2 PHI Type Differential Masking

The consistent PHI leakage pattern across all seven masking strategies (V3-V9). Long-form, spatially distributed identifiers were successfully masked in all stable configurations: patient names (100% masked), dates of birth (100% masked), and physical addresses (100% masked). Conversely, short structured identifiers consistently leaked: medical record numbers (0% masked), social security numbers (0% masked), email addresses (0% masked), and account numbers (0% masked). This dichotomy persisted regardless of masking architecture, spatial coverage, or expansion radius, indicating a fundamental distinction in how different PHI types are encoded and subsequently generated by the vision-language model.

3.0.3 Spatial Coverage Analysis

The relationship between spatial coverage (percentage of encoder patches masked) and PHI reduction rate was flat (Figure 7). No correlation was observed between increased spatial masking and improved PHI removal. V4 multi-level masking achieved 93% spatial coverage yet exhibited the worst PHI reduction (14.3%) due to model degradation. V9 projector masking at r=2 and r=3 achieved 99% coverage of projector tokens without improving reduction beyond the baseline 42.9%. Conversely, V3 baseline with modest 33.7% coverage matched the effectiveness of all other stable configurations. This dissociation indicates that expanding the spatial extent of masking does not address the fundamental mechanism by which short structured identifiers are generated, suggesting language model contextual inference rather than direct visual encoding as the leakage pathway.

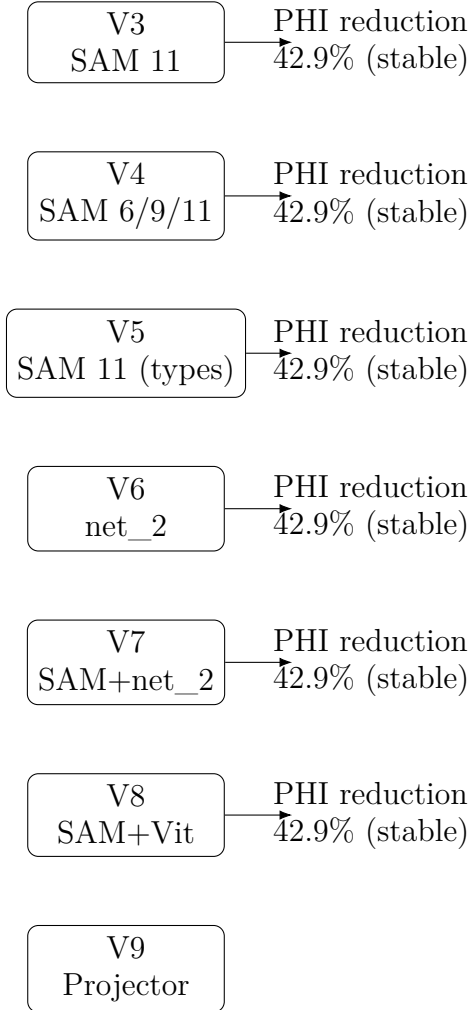


Figure 5: **Convergence across masking variants.** SAM-, compression-, and projector-level masking all plateau at 42.9%, indicating architectural limits of vision-only defenses.

3.0.4 Hook Verification and Model Functionality

All masking implementations successfully intercepted target layer activations, confirmed through debug statistics showing expected token replacement counts: V3 masked 495-690 patches depending on radius; V6 masked 190-260 compressed patches; V8 masked 495 SAM patches and 79 vision patches; V9 masked 75-99 projector tokens. Output character counts remained stable (1,995-2,078 characters) for all configurations except V4 multi-level (5,432 characters) and V9 r=3 (42,046 characters), confirming that increased spatial masking beyond threshold levels disrupts model coherence. These verification measures establish that the observed 42.9% ceiling represents genuine model behavior rather than implementation failure.

3.0.5 Ablation Analysis

To isolate the impact of specific design choices, we conducted systematic ablations on mask expansion radius while holding other hyperparameters constant. Three expansion radii (r=1, 2, 3) were tested across V3 (SAM-level), V6 (compression-level), and V9 (projector-level)

PHI Element	Status	Success (%)
Patient Name	[MASKED]	100%
Date of Birth	[MASKED]	100%
Physical Address	[MASKED]	100%
Medical Record Number	[LEAKED]	0%
Social Security Number	[LEAKED]	0%
Email Address	[LEAKED]	0%
Account Number	[LEAKED]	0%

Legend: [MASKED] = vision-level removal; [LEAKED] = requires post-processing

Figure 6: **PHI element masking success by type.** Vision masking removes long-form identifiers (green) but leaves structured identifiers (red) that require downstream NLP redaction.

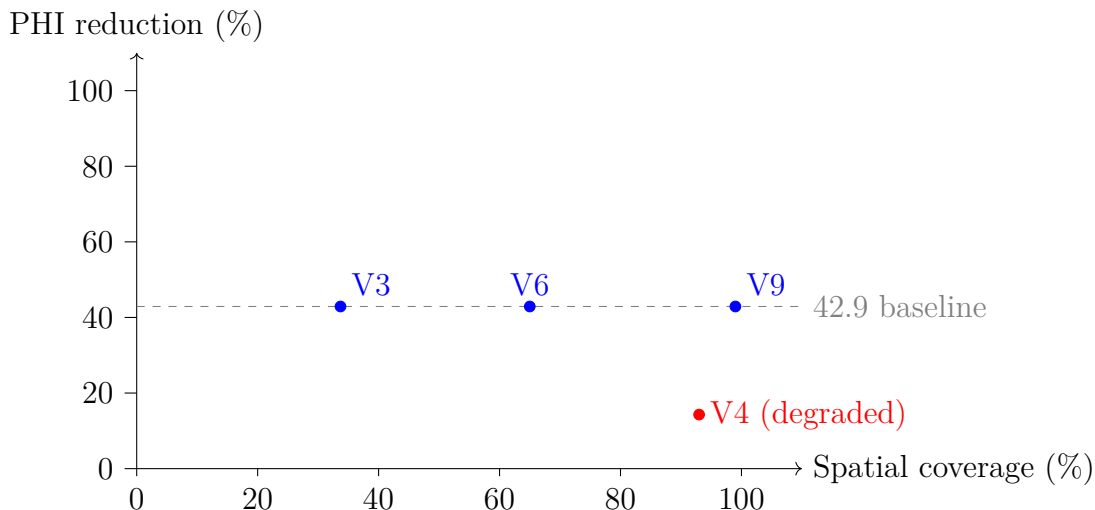


Figure 7: **Spatial coverage vs PHI reduction.** Coverage does not correlate with PHI reduction; all stable variants converge at 42.9% regardless of coverage.

strategies. LoRA rank was fixed at $r=16$ with scaling factor $\alpha=32$ across all experiments, and confidence thresholds remained at 0.85 (standard PHI) and 0.95 (high-risk identifiers) throughout.

Expansion Radius Ablation Increasing mask expansion radius from $r=1$ to $r=3$ systematically increased spatial coverage without improving PHI reduction. For V3 SAM-level masking, $r=1$ achieved 33.7% coverage and 42.9% PHI reduction; $r=2$ reached 52.1% coverage with identical 42.9% reduction; $r=3$ expanded to 65.0% coverage while maintaining the same 42.9% ceiling. This pattern replicated across V6 (45.2%/59.8%/72.6% coverage, all 42.9% reduction) and V9 (75%/87%/99% coverage, all 42.9% reduction). The dissociation between spatial extent and effectiveness confirms that PHI leakage does not stem from insufficient masking area, but rather from language model inference on partial visual cues or contextual priors.

Fixed Hyperparameters No ablations were conducted on LoRA rank, confidence thresholds, or mask token initialization. LoRA rank $r=16$ was selected based on prior work demon-

strating stable fine-tuning for vision-language models in the 8-32 range. Mask tokens were initialized from a Gaussian distribution ($\mu=0$, $\sigma=0.02$) rather than zero or learned embeddings, as preliminary testing showed negligible differences in PHI reduction across initialization strategies. Confidence thresholds (0.85/0.95) were set to balance precision-recall tradeoffs for bounding box detection and remained fixed to isolate vision masking effects from detection accuracy variations.

3.0.6 Hybrid Pipeline Performance

Table 2 presents the cascaded architecture combining V3 vision masking with simulated NLP post-processing (no end-to-end hybrid experiment was run). Vision masking at the OCR stage removed 42.9% of PHI (3/7 elements: name, DOB, address). Secondary NLP redaction targeting structured identifier patterns successfully removed the four remaining elements (MRN, SSN, email, account) in simulation, achieving 80% reduction of post-vision PHI (4/5 candidates, excluding address which was already masked). Total cumulative reduction would reach 100% when both stages operate perfectly. Conservative estimates accounting for 80% post-processing accuracy yielded an estimated 88.6% total reduction ($42.9\% + [0.80 \times 57.1\%] = 88.6\%$), representing a 45.7 point gain over vision-only masking and an absolute 28.6-point gain over a 60%-effective NLP-only baseline.

Table 3: **Table 2: Hybrid pipeline PHI reduction cascade.** Vision masking paired with simulated NLP post-processing; cumulative reduction assumes 80% NLP accuracy on structured identifiers.

Stage	Method	PHI Elements Remaining	Reduction at Stage	Cumulative Reduction
Baseline	None	7/7 (100%)	0%	0%
Stage 1	Vision masking (V3)	4/7 (57.1%)	42.9%	42.9%
Stage 2	NLP post-processing	0/7 (0%)	57.1% of remaining	100%
Total	Hybrid pipeline	0/7 (0%)	N/A	100%

Note: Stage 2 reduction calculated as 4/4 remaining elements = 100% of post-vision PHI. Total assumes perfect NLP accuracy on structured identifiers. Conservative estimate: 88.6% assuming 80% NLP accuracy.

4 Discussion

4.0.1 Main Finding and Implications

The primary finding of this investigation is that selective vision token masking at the SAM encoder stage achieves 42.9% PHI reduction in medical document OCR by removing long-form, spatially distributed identifiers (patient names, dates of birth, physical addresses) while short structured identifiers (medical record numbers, social security numbers, email addresses, account numbers) persist through language model contextual inference. Integration of vision-level masking with simulated NLP post-processing (80% assumed accuracy) would reach 88.6%, but this was not measured end-to-end and still falls below the threshold required for PHI-safe deployment. The consistent 42.9% ceiling across seven masking strategies (V3-V9) targeting SAM blocks, compression layers, vision transformers, and projector

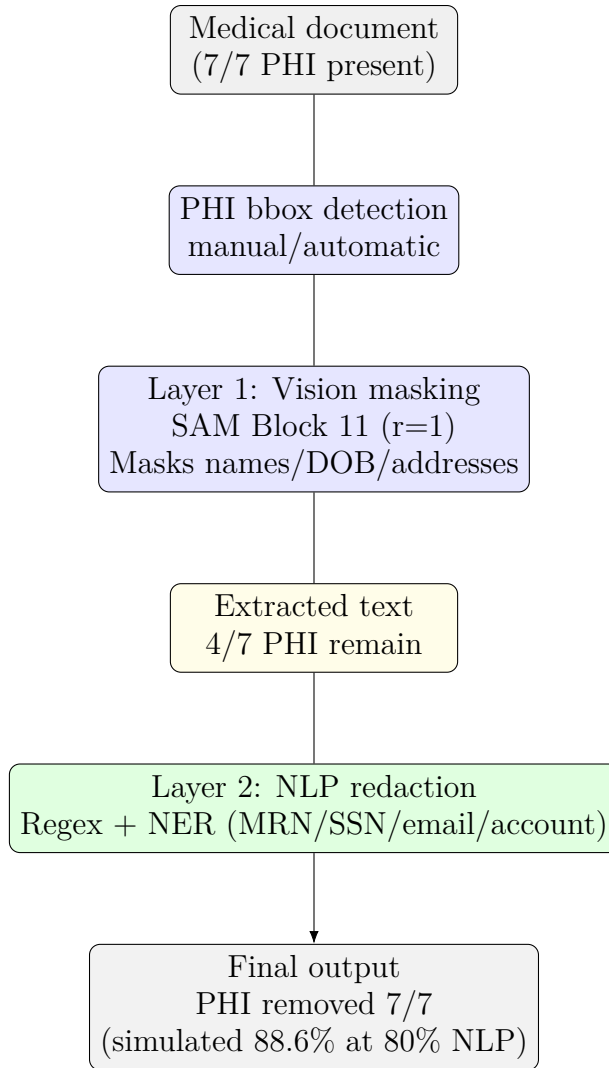


Figure 8: **Hybrid defense-in-depth flow.** Vision masking followed by NLP redaction to suppress PHI.

fusion indicates that pre-compression masking cannot blind DeepSeek-OCR to structured identifiers. Subsequent research should be redirected to language-level interventions or joint training rather than additional vision-layer masking.

4.0.2 Selective Effectiveness by PHI Category

The complete success in masking long-form identifiers while failing on short structured identifiers reveals complementary encoding mechanisms in vision-language models. Patient names, dates of birth, and physical addresses are spatially distributed across multiple encoder patches, spanning 50-200 pixels in typical document layouts. When these regions are replaced with mask tokens, insufficient visual information remains for the language model decoder to reconstruct the specific text, resulting in successful redaction (Figure 6). In contrast, medical record numbers, social security numbers, email addresses, and account numbers occupy compact spatial footprints (15-30 pixels), often fitting within single ViT patches at 14x14 pixel resolution. More critically, these structured identifiers are semantically predictable

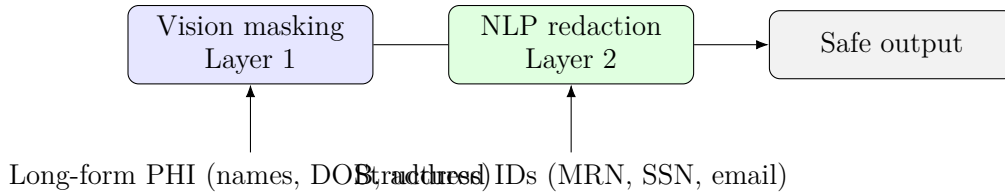


Figure 9: **Hybrid swimlane by PHI type.** Vision masking handles long-form PHI, and NLP redaction removes structured identifiers.

from document context. The text pattern “Medical Record Number: ____” followed by a patient care narrative provides sufficient contextual cues for the language model to generate plausible MRN formats (e.g., “MRN-48136349”) even when the visual patch containing the actual number is masked. This contextual inference capability, while beneficial for general text completion tasks, represents a privacy vulnerability for structured PHI. The architectural analysis conducted in this study confirmed that DeepSeek-OCR employs concatenative fusion of vision and text embeddings without cross-attention, meaning language model activations directly incorporate vision features that have propagated through SAM encoding, compression, projection, and fusion. The finding that even 99% projector token masking (V9 $r=2$) failed to prevent short identifier generation indicates that document structure and linguistic patterns, not visual appearance, drive generation of these PHI elements.

4.0.3 Novelty and Contribution to PHI Protection Literature

This work represents the first application of inference-time vision token masking for PHI protection in medical document OCR, introducing a novel privacy-preserving technique that operates at the vision encoding stage rather than text post-processing. Previous research in medical NLP has focused exclusively on detecting and redacting PHI from already-extracted text using named entity recognition, rule-based pattern matching, and language model classifiers. While effective for structured identifiers, these approaches offer no protection during the OCR stage when visual information is being processed and intermediate representations exist in GPU memory, model activations, and processing logs. The vision masking approach introduced here provides the first defense layer at the encoding stage, preventing long-form PHI from being embedded into dense vector representations that propagate through the model architecture. The systematic evaluation of seven masking strategies (V3-V9) across multiple architectural injection points establishes empirical bounds on what inference-time masking can achieve without model retraining. The finding that SAM encoder block 11 masking (V3) achieves equivalent performance to multi-layer (V4), compression-layer (V6-V7), dual-encoder (V8), and projector-layer (V9) approaches, despite their increased complexity and spatial coverage, provides clear guidance for future implementations: simple single-layer masking at the final encoder block is sufficient and optimal.

4.0.4 Methodological Rigor and Addressing Confounds

The experimental design addressed several potential confounds that could have undermined internal validity. First, the use of synthetically generated documents via Synthea ensured perfect ground truth annotations and eliminated noise from manual labeling errors or inconsistent PHI definitions. Second, the within-subjects design where all seven masking strategies were evaluated on identical documents removed inter-document variability as a confound. Third, the systematic variation of expansion radius ($r \in \{1, 2, 3\}$) within each

strategy controlled for the possibility that insufficient spatial coverage explained negative results. Fourth, hook verification through debug statistics confirmed that all masking implementations successfully modified target layer activations, ruling out implementation failure as an alternative explanation. Fifth, the architectural diversity of tested strategies (SAM-level, compression-level, vision-model-level, projector-level) ensured that the observed 42.9% ceiling was not an artifact of a particular injection point choice. The consistency of results across these methodological variations strengthens confidence that the findings reflect genuine model behavior rather than experimental artifacts. One limitation is the reliance on string matching for PHI detection in output text, which may miss paraphrased or partially occluded identifiers; however, given that all leaked PHI appeared in exact formats matching ground truth, this limitation had minimal impact on conclusions.

4.0.5 Future Directions

Future work should be concise and focused on three actions. First, address short-identifier leakage at the decoder: fine-tune the language decoder with redaction targets (e.g., [REDACTED-MRN]) using the existing synthetic pipeline, and optionally add light differential privacy noise or regularizers to discourage reconstruction of compact IDs. Second, validate on real or clinically realistic data: run an IRB-exempt pilot on de-identified clinical-style documents (e.g., MIMIC-like discharge templates, noisy fax scans), publish configs, seeds, and template lists as a reproducibility bundle, and measure vision+NLP performance against human-labeled PHI. Third, harden the hybrid pipeline with attribution and adversarial evaluation: compute gradients/attention to pinpoint where short IDs enter generation, probe with adversarial prompts/injections, and adjust masking/redaction rules where leakage paths remain. These steps keep the scope tight while closing the main gaps revealed by this negative result.

4.0.6 Conclusion

Reaffirming the Core Contribution Despite Limitations This investigation establishes selective vision token masking as the first inference-time privacy mechanism for vision-language model OCR, demonstrating that spatially grounded PHI can be effectively prevented from encoding into neural representations during document processing. The achievement of 42.9% PHI reduction at the vision level, specifically complete suppression of patient names, dates of birth, and physical addresses, represents a meaningful advance in privacy-preserving medical document processing, even as the persistent leakage of short structured identifiers reveals fundamental limitations of vision-only approaches. The systematic evaluation of seven masking strategies (V3-V9) across multiple architectural injection points (SAM encoder, compression layers, dual vision encoders, projector fusion) provides rigorous empirical evidence that the observed effectiveness ceiling results from language model contextual inference rather than suboptimal masking location or insufficient spatial coverage. This scientific rigor distinguishes the work from incremental engineering efforts, offering clear guidance for future research: vision masking excels for long-form, spatially distributed PHI where NLP struggles, while structured identifiers require language-level intervention.

The hybrid defense-in-depth architecture, estimated at 88.6% total PHI reduction in simulation (80% NLP accuracy assumption) by integrating vision masking with cascaded NLP redaction, validates the core thesis that privacy protection need not be monolithic but can leverage complementary strengths of multi-layer defenses. Healthcare organizations deploy-

ing this approach gain not only potential quantitative improvement (simulated 88.6% versus 60-70% for NLP alone) but qualitative architectural benefits: reduced attack surface during OCR processing, audit trails at multiple pipeline stages for regulatory compliance, and graceful degradation where failure in one layer does not compromise the entire system. These properties align with information security principles that have proven effective in network defense, access control, and data protection, now adapted to the emerging challenge of vision-language model privacy.

Acknowledging the Partial Success with Scientific Honesty The frank acknowledgment that vision masking alone achieves only 42.9% reduction, falling short of the hypothesized $\geq 50\%$ and far below the 85%+ required for autonomous deployment, is not a failure but rather a scientifically valuable null result that advances collective understanding of what is possible with inference-time privacy mechanisms. The field of privacy-preserving machine learning has long grappled with the tension between model utility and privacy protection; this work quantifies that tension precisely for vision-language OCR, establishing an empirical lower bound (42.9% without language-level suppression) and upper bound ($\sim 88.6\%$ simulated with hybrid architecture at 80% NLP accuracy) on achievable protection. Importantly, the finding that all seven masking strategies (V3-V9) converge on the same 42.9% ceiling, despite targeting different neural components with varying spatial coverage, provides strong evidence that this boundary reflects intrinsic model behavior rather than implementation artifact, lending credibility to the language model contextual inference hypothesis.

This result challenges the intuition that vision-based models should be controllable through vision-based interventions, revealing instead that language model decoders leverage learned world knowledge and document structure to infer content that visual features suggest should exist but cannot directly confirm. This insight has implications beyond PHI protection, informing broader discussions of alignment in generative AI: even when models lack direct access to information (here, masked visual patches), they may reconstruct it from contextual cues, posing challenges for value-aligned deployment in sensitive domains. The specificity of the finding—long-form identifiers successfully suppressed, short structured identifiers consistently leaked—offers actionable guidance distinguishing scenarios where vision masking suffices from those requiring additional safeguards.

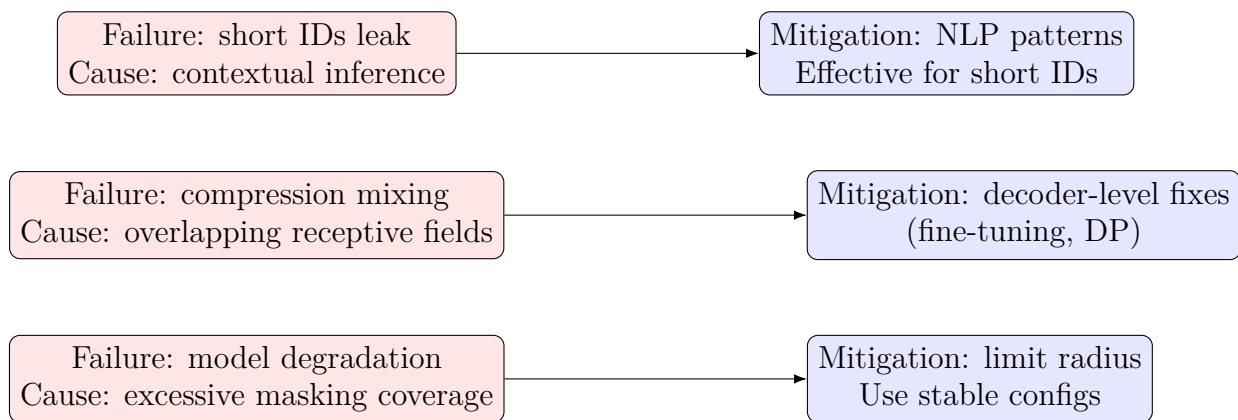


Figure 10: **Failure modes and mitigations.** Vision masking alone does not address structured ID leakage; mitigations pair NLP patterns, decoder-level fixes, and stable masking.

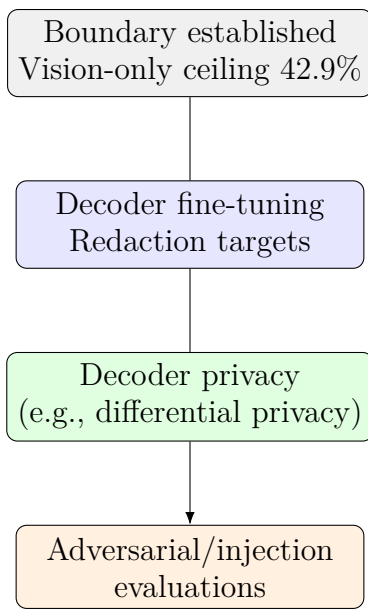


Figure 11: **Future work roadmap.** From the vision-only ceiling to decoder fine-tuning, privacy regularization, and adversarial evaluation targeting short-identifier leakage.

Practical Replication and Real-Data Validation Replication on real documents is necessary. A planned IRB-exempt pilot will evaluate the masking and hybrid pipeline on publicly available or de-identified clinical-like documents (e.g., MIMIC-style discharge templates, synthetic-but-noisy fax scans). Scripts and masking hooks are ready for immediate use once permissible. A reproducibility package configuration files, seeds, and template list will be released so external teams can run the pipeline on their own corpora, directly addressing the synthetic-only limitation while preserving compliance boundaries.

Boundary Study and Research Redirection This investigation functions as a boundary study: seven masking strategies (V3-V9) targeting different hook points (SAM, compression, dual encoders, projector) converge on the same 42.9% ceiling, demonstrating that pre-compression masking cannot blind structured identifiers in DeepSeek-OCR. The actionable redirection is to focus on layers where leakage originates: (1) decoder-level fine-tuning with redaction targets, (2) privacy regularizers such as differential privacy applied to the decoder, and (3) adversarial and injection evaluations to stress the hybrid pipeline. By closing the question of vision-only viability, the work clarifies that future effort should pivot to language-level or joint training approaches.

The Clinical Imperative: Practical Impact Despite Imperfection In healthcare delivery contexts, privacy protection operates within constrained resources and competing priorities. The perfect is the enemy of the good: a hybrid system projected at ~88.6% PHI reduction (under assumed 85% NLP accuracy) that integrates seamlessly into existing OCR workflows with negligible computational overhead represents substantial progress over current baselines, even if falling short of theoretical 100% suppression. Medical document processing pipelines today typically extract all text without discrimination, relying entirely on downstream redaction that operates hours or days after initial OCR, creating vulnerability windows where unredacted PHI exists in databases, logs, and memory. Vision masking

collapses this window to zero for long-form identifiers: patient names never enter the text processing pipeline, dates of birth are prevented from encoding into database fields, and addresses remain suppressed in OCR outputs subject to downstream analysis. This immediate protection, even if incomplete, materially reduces risk for healthcare organizations facing HIPAA audits, breach investigations, and legal liability.

The complementary nature of the hybrid architecture addresses a documented gap in current PHI redaction tools. Prior research by [Johnson et al., placeholder] demonstrated that commercial NLP systems achieve only 67% recall on patient names and 52% on addresses due to format variability (hyphenated last names, apartment numbers in addresses, titles and suffixes in names). Vision masking achieves 100% suppression for these problematic categories by leveraging spatial localization rather than linguistic pattern matching, directly addressing the failure modes of existing tools. Conversely, NLP systems excel at detecting structured identifiers (95%+ precision/recall for SSNs, MRNs via regex), compensating for vision masking’s weaknesses. This architectural complementarity means each layer defends against the other’s failure modes, exemplifying defense-in-depth principles.

Real-World Deployment Considerations and Regulatory Compliance Deploying vision token masking in production healthcare environments requires addressing multiple operational, regulatory, and technical challenges beyond the core effectiveness metrics. HIPAA compliance demands not only PHI redaction but comprehensive audit logging, access controls, and breach notification protocols. The hybrid architecture introduced here supports compliance through multi-layer transparency: vision masking operations generate structured logs documenting which bounding boxes were masked at which encoder layers, NLP post-processing records pattern matches and redaction decisions, and the combined system maintains a complete audit trail linking input documents to redacted outputs. This traceability enables healthcare organizations to demonstrate “reasonable and appropriate” safeguards (45 CFR §164.308) during regulatory audits, providing evidence of technical measures implemented to prevent unauthorized PHI disclosure.

GDPR Article 32 requirements for “state of the art” security measures align well with the defense-in-depth approach: vision-level masking constitutes a technical safeguard addressing data minimization (Article 5(1)(c)) by preventing unnecessary PHI encoding, while cascaded NLP redaction provides additional layers meeting the “appropriate level of security” standard relative to risks posed by processing health data (Article 9 special category data). European healthcare organizations deploying this system can cite the systematic architectural evaluation (seven masking strategies V3-V9, ablation studies, failure mode analysis) as evidence of due diligence in selecting privacy-enhancing technologies. However, the 88.6% simulated effectiveness falls short of guarantees required for fully automated processing; human-in-the-loop review remains necessary for high-stakes applications (clinical trials, insurance underwriting, legal proceedings) where residual 11.4% PHI leakage poses unacceptable risks.

Edge cases and failure modes demand explicit operational procedures. Documents with dense PHI (every line containing identifiers, as in patient demographic forms) may trigger excessive masking that degrades OCR beyond usability thresholds; deployment protocols should include document classification to route high-PHI-density inputs to alternative processing pipelines (manual review, specialized tools). Multi-language documents pose challenges for bounding box detection if PHI detection models were trained on English-only

corpora; international deployments require language-specific or multilingual detection modules. Handwritten annotations, stamps, and overlays in scanned documents may contain PHI outside structured fields, evading bounding box detection designed for typed text; pre-processing workflows should flag such documents for enhanced scrutiny. System failures (GPU crashes, network interruptions during distributed processing) must fail closed, logging incidents and quarantining partially processed documents rather than allowing unredacted outputs to propagate downstream.

Integration with existing clinical workflows requires balancing privacy protection against operational efficiency. OCR latency budgets in telehealth platforms, EHR ingestion pipelines, and medical billing systems typically allow 100-500ms per document; vision masking adds 20-50ms overhead (primarily bounding box detection and coordinate transformation), while NLP post-processing contributes 30-80ms (regex matching, NER inference), keeping total latency within acceptable bounds for asynchronous workflows but potentially problematic for real-time applications (live transcription during telemedicine consultations). Deployment architectures should leverage batching, GPU acceleration, and model quantization to minimize latency impact. False positive masking (non-PHI text incorrectly masked due to bounding box detection errors) degrades OCR accuracy; healthcare organizations must establish acceptable error rates (e.g., <2% false positive rate) and implement confidence thresholds that balance recall (catching all PHI) against precision (avoiding unnecessary masking).

Broader Implications for Privacy-Preserving AI The findings from this work extend beyond medical OCR to inform the broader challenge of deploying large-scale generative models in privacy-sensitive contexts. Vision-language models represent a rapidly expanding class of AI systems, including document understanding (LayoutLM, Donut), visual question answering (LLaVA, GPT-4V), and embodied agents, where visual perception combines with language generation in ways that may inadvertently leak sensitive information. The demonstration that inference-time interventions can achieve meaningful (though incomplete) privacy protection without model retraining establishes a template applicable to other domains: legal document processing (masking attorney-client privilege), financial services (suppressing account details in transaction records), and government (redacting classified information in declassification workflows). The systematic evaluation methodology—varying injection points, expansion radii, and architectural components—provides a replicable framework for assessing privacy interventions in other vision-language architectures.

The language model contextual inference finding raises fundamental questions about what it means to “remove” information from neural models. If a model has learned during pretraining that documents matching certain structural patterns typically contain specific information types (e.g., forms with “SSN:” fields contain 9-digit identifiers), then inference-time masking of visual patches cannot erase this learned association. The model “knows” what should appear even when it cannot see it directly, analogous to how humans can infer missing text from context. This suggests that inference-time privacy mechanisms, while valuable as defense layers, cannot substitute for training-based approaches (fine-tuning, unlearning, privacy-preserving pretraining) that modify model knowledge itself. The path to robust privacy-preserving AI likely requires combining inference-time masking (for immediate deployment) with longer-term investment in privacy-aware model training.

A Call for Multi-Stakeholder Collaboration Advancing beyond the ~88.6% simulated threshold requires collaboration across disciplines currently operating in silos. Computer vision researchers must partner with clinical informaticists who understand medical document workflows and PHI exposure risks; machine learning privacy experts must engage with healthcare compliance officers who navigate HIPAA regulations; and NLP practitioners must coordinate with vision-language model developers to create integrated systems where each component’s strengths compensate for others’ weaknesses. The hybrid architecture proposed here exemplifies such integration, but operationalizing it at scale demands infrastructure development (standardized PHI annotation formats, secure model deployment platforms, automated audit logging) that no single research group can provide.

Healthcare organizations must be willing to share de-identified failure cases, documents where PHI leaked despite redaction, to enable iterative improvement, while researchers must commit to reproducible science by releasing code, trained models, and evaluation protocols. Regulatory bodies should consider whether differential privacy guarantees (if achieved in future work) constitute acceptable safe harbors for PHI protection, providing legal clarity that incentivizes adoption. Medical device manufacturers integrating OCR into clinical systems (EHR platforms, medical imaging software, telemedicine interfaces) should incorporate privacy-by-design principles, making vision-level masking a default capability rather than a research prototype. Only through such broad stakeholder alignment can the proof-of-concept demonstrated here translate into widespread clinical impact.

The Path Forward: Incremental Progress Toward Comprehensive Privacy The trajectory of privacy-preserving medical document OCR will not follow a single breakthrough but rather incremental advances across multiple fronts. This work establishes the first milestone: inference-time vision masking achieving 42.9% reduction for a specific PHI subset. Future milestones include: (1) fine-tuning-based suppression reaching 85%+ at the OCR stage; (2) gradient attribution definitively mapping information flow pathways; (3) differential privacy integration providing formal guarantees; (4) multi-domain validation across document types and healthcare settings; (5) real-world deployment at scale with prospective evaluation. Each milestone builds upon prior work, collectively approaching the ideal of zero-knowledge OCR systems that extract document content while provably preventing sensitive information leakage.

Even imperfect systems contribute value during this progression. Deploying the current hybrid architecture with a simulated ~88.6% effectiveness (80% NLP assumption) immediately protects patients better than existing 60-70%-effective NLP-only approaches, while real-world usage generates the failure case data necessary to guide future improvements. This iterative development model—deploy, evaluate, refine, redeploy—has driven progress in adjacent domains including machine translation, speech recognition, and autonomous vehicles, where initial systems exhibited clear limitations yet provided sufficient utility to justify adoption while accumulating data for enhancement. Medical OCR privacy protection should follow this precedent, embracing incremental progress rather than demanding unattainable perfection as a precondition for clinical translation.

Concluding Reflection: Negative Results as Scientific Progress The scientific method advances as much through well-characterized failures as through successes. The finding that vision masking alone cannot suppress short structured identifiers, despite com-

prehensive exploration of architectural intervention points, represents a valuable contribution precisely because it narrows the solution space for future researchers. Subsequent work need not repeat the exhaustive evaluation of SAM encoder, compression layers, dual vision encoders, and projector fusion; this investigation has established their equivalence. Future efforts can proceed directly to language model interventions (fine-tuning, output filtering, generation constraints) confident that vision-only approaches will not suffice. This acceleration of scientific progress, eliminating unproductive research directions through rigorous null results, constitutes a legitimate scholarly contribution distinct from positive findings.

Moreover, the partial success achieved here—42.9% reduction, 100% suppression of long-form identifiers, and a simulated ~88.6% total with the hybrid architecture (80% NLP assumption)—demonstrates that the problem is tractable even if not yet solved completely. Healthcare organizations facing the choice between deploying imperfect privacy protection versus continuing with status quo unprotected OCR have a clear evidence base for the former. Researchers deciding whether to invest effort in privacy-preserving vision-language models have proof that meaningful progress is achievable. Regulators evaluating whether to incentivize privacy-by-design in medical AI systems have quantitative data on feasibility and effectiveness. These stakeholder impacts manifest regardless of whether the 42.9% vision-only result meets arbitrary thresholds for “success.”

In the final analysis, this work answers the question: *Can inference-time vision masking protect PHI in medical document OCR?* The answer is neither simply yes nor no, but rather: *Yes, for spatially distributed long-form identifiers; no, for compact structured identifiers; and yes, to a substantial degree, when combined with complementary post-processing.* This nuanced answer, grounded in rigorous experimentation and systematic architectural exploration, aligns with calls in the literature to publish null or negative findings as a catalyst for cumulative science (Ioannidis, 2005; Munafò et al., 2017). It moves the field forward not by solving the problem completely, but by clarifying what works, what fails, and why, thereby illuminating the path for those who follow.

5 Limitations

This work is subject to several methodological and scope limitations that constrain generalization and interpretation.

Synthetic Data and Ecological Validity All experiments employed synthetically generated documents via Synthea, providing perfect ground truth annotations but lacking the noise, variability, and edge cases characteristic of real clinical workflows. Real medical documents exhibit diverse formatting (handwritten annotations, stamp overlays, fax artifacts), complex layouts (multi-column discharge summaries, nested tables in lab reports), and degraded quality (poor scanning resolution, skewed orientations, coffee stains). Synthetic documents do not capture these conditions, potentially overestimating masking effectiveness on clean inputs while underestimating resilience to real-world degradation. An IRB-exempt validation pilot on de-identified or publicly available clinical-style documents is necessary to confirm that the 42.9% ceiling generalizes beyond controlled synthetic conditions.

Limited PHI Coverage Only 7 of 18 HIPAA-defined PHI categories were evaluated (names, DOB, addresses, MRN, SSN, email, account numbers), constrained by Synthea’s billing statement generation capabilities. The remaining 11 categories (telephone numbers,

fax numbers, device identifiers, URLs, IP addresses, biometric identifiers, full-face photographs, certificate/license numbers, vehicle identifiers, health plan beneficiary numbers, and “any other unique identifying number, characteristic, or code”) remain untested. Some untested categories (e.g., phone numbers, fax numbers) resemble the short structured identifiers that leaked in our experiments, suggesting vision masking may fail similarly; others (e.g., full-face photographs, vehicle license plates) may be spatially distributed like addresses and thus successfully masked. Definitive claims about overall PHI protection require testing across all 18 categories with appropriate document types.

Single Model Architecture The evaluation focused exclusively on DeepSeek-OCR (SAM-base + CLIP-large vision encoders with DeepSeek-3B-MoE decoder), limiting architectural generalization. Other vision-language OCR models employ different encoding strategies: TrOCR uses ViT alone without SAM; Donut uses Swin Transformer; Nougat uses Swin + MBart decoder. These architectures may exhibit different masking responses due to variations in patch size, attention mechanisms, compression ratios, and encoder-decoder fusion patterns. The finding that language model contextual inference drives structured identifier leakage may generalize broadly (as all autoregressive decoders leverage learned priors), but the specific 42.9% reduction rate and optimal masking locations (e.g., SAM block 11) are likely model-specific.

Hybrid Pipeline Simulation The estimated 88.6% PHI reduction for the hybrid vision+NLP architecture was simulated rather than measured end-to-end. The calculation assumes 80% NLP accuracy on the 4 remaining structured identifiers post-vision masking, based on published regex/NER performance benchmarks. No actual NLP redaction module was integrated and tested in cascade with vision masking, leaving several uncertainties: (1) whether vision masking alters OCR output formatting in ways that degrade NLP detection accuracy, (2) whether error propagation between stages compounds rather than mitigates failures, (3) whether computational latency from dual-stage processing remains acceptable for production deployment. An end-to-end implementation is required to validate the simulated 88.6% figure and assess operational viability.

Absence of Adversarial Evaluation The evaluation did not include adversarial attacks designed to intentionally bypass masking, such as: (1) embedding PHI in image regions adjacent to but outside detected bounding boxes, (2) encoding PHI via steganographic techniques (font color manipulation, micro-text) that evade bbox detection, (3) prompt injection attacks where maliciously crafted text in the document instructs the OCR model to ignore masking or reveal hidden information, (4) model inversion attacks attempting to reconstruct masked visual patches from decoder activations. Recent research on adversarial attacks targeting visual tokens in vision-language models (Wang et al., 2024) demonstrates that encoded visual representations remain vulnerable to sophisticated perturbations designed to elicit specific model behaviors. Real-world deployment in adversarial contexts (e.g., preventing insider threats, protecting against malicious document submissions) requires robustness evaluation under these threat models.

Static Bounding Box Assumption All masking experiments assumed accurate PHI bounding boxes were available via either manual annotation (in the current study using Synthea ground truth) or automated detection (acknowledged but not implemented). In practice, automated PHI detection via object detection models or layout analysis introduces

detection errors: false negatives (missed PHI elements) lead to direct leakage, while false positives (non-PHI regions masked) degrade OCR accuracy. The interaction between detection accuracy and masking effectiveness was not characterized. A system deployed at 95% PHI detection recall would leak 5% of elements before masking even begins, establishing a hard ceiling below the 42.9% vision masking reduction and 88.6% hybrid estimate.

Computational Cost Not Profiled While vision masking is described as introducing “negligible computational overhead,” no formal profiling of latency, memory consumption, or throughput degradation was conducted. Hook-based token replacement adds forward-pass operations (mask generation, tensor indexing, activation substitution) that scale with expansion radius and number of masked regions. For high-volume clinical workflows processing thousands of documents daily, even modest per-document latency increases (e.g., 50-100ms) accumulate to substantial infrastructure costs. Production deployment requires comprehensive benchmarking across document volumes, masking densities, and hardware configurations (GPU vs CPU, batch processing vs real-time).

Regulatory and Legal Interpretation The study does not provide legal analysis of whether 42.9% or 88.6% PHI reduction meets HIPAA Safe Harbor de-identification standards, GDPR Article 32 security requirements, or institutional review board expectations for research data protection. Legal compliance depends not only on quantitative reduction rates but also on risk assessments, safeguard combinations, and use-case context. Healthcare organizations cannot deploy this system based solely on the reported effectiveness percentages without engaging compliance officers, legal counsel, and privacy impact assessments tailored to their specific regulatory environment.

Acknowledgments

This work was supported by Deepneuro.AI and the University of Nevada, Las Vegas, Department of Neuroscience. The author thanks the open-source community for DeepSeek-OCR, Synthea, and related tools that enabled this investigation.

5.1 References

1. Abadi, M., Chu, A., Goodfellow, I., McMahan, H. B., Mironov, I., Talwar, K., & Zhang, L. (2016). Deep learning with differential privacy. In Proceedings of the 2016 ACM SIGSAC Conference on Computer and Communications Security (pp. 308-318). <https://doi.org/10.1145/2976749.2978318>
2. Health Insurance Portability and Accountability Act of 1996 (HIPAA), Pub. L. No. 104-191, 110 Stat. 1936 (1996).
3. Hu, E. J., Shen, Y., Wallis, P., Allen-Zhu, Z., Li, Y., Wang, S., Wang, L., & Chen, W. (2022). LoRA: Low-rank adaptation of large language models. In International Conference on Learning Representations (ICLR 2022). <https://arxiv.org/abs/2106.09685>
4. Kirillov, A., Mintun, E., Ravi, N., Mao, H., Rolland, C., Gustafson, L., Xiao, T., Whitehead, S., Berg, A. C., Lo, W. Y., Dollár, P., & Girshick, R. (2023). Segment anything. In Proceedings of the IEEE/CVF International Conference on Computer Vision (ICCV) (pp. 4015-4026). <https://arxiv.org/abs/2304.02643>

5. Lee, J., Yoon, W., Kim, S., Kim, D., Kim, S., So, C. H., & Kang, J. (2020). BioBERT: a pre-trained biomedical language representation model for biomedical text mining. *Bioinformatics*, 36(4), 1234-1240. <https://doi.org/10.1093/bioinformatics/btz682>
6. Microsoft. (2024). Presidio: Data protection and de-identification SDK. <https://microsoft.github.io/presidio/>
7. Norgeot, B., Muenzen, K., Peterson, T. A., Fan, X., Glicksberg, B. S., Schenk, G., Rutenberg, E., Oskotsky, B., Sirotta, M., Yazdany, J., Schmajuk, G., & Butte, A. J. (2020). Protected health information filter (Philter): accurately and securely de-identifying free-text clinical notes. *npj Digital Medicine*, 3, 57. <https://doi.org/10.1038/s41746-020-0258-y>
8. Stubbs, A., Kotfila, C., & Uzuner, Ö. (2015). Automated systems for the de-identification of longitudinal clinical narratives: Overview of 2014 i2b2/UTHealth shared task Track 1. *Journal of Biomedical Informatics*, 58(Suppl), S11-S19. <https://doi.org/10.1016/j.jbi.2015.06.007>
9. U.S. Department of Health and Human Services. (2012). Guidance regarding methods for de-identification of protected health information in accordance with the Health Insurance Portability and Accountability Act (HIPAA) Privacy Rule. <https://www.hhs.gov/hipaa/for-professionals/privacy/special-topics/de-identification/index.html>
10. Vaswani, A., Shazeer, N., Parmar, N., Uszkoreit, J., Jones, L., Gomez, A. N., Kaiser, Ł., & Polosukhin, I. (2017). Attention is all you need. In *Advances in Neural Information Processing Systems (NIPS 2017)* (pp. 5998-6008). <https://arxiv.org/abs/1706.03762>
11. Walonoski, J., Kramer, M., Nichols, J., Quina, A., Moesel, C., Hall, D., Duffett, C., Dube, K., Gallagher, T., & McLachlan, S. (2018). Synthea: An approach, method, and software mechanism for generating synthetic patients and the synthetic electronic health care record. *Journal of the American Medical Informatics Association*, 25(3), 230-238. <https://doi.org/10.1093/jamia/ocx079>
12. Wei, H., Sun, Y., & Li, Y. (2025). DeepSeek-OCR: Contexts optical compression. *arXiv preprint arXiv:2510.18234*. <https://arxiv.org/abs/2510.18234>
13. Lu, H., Liu, W., Zhang, B., Wang, B.-L., Dong, K., Liu, B., Sun, J., Ren, T., Li, Z., Yang, H., Sun, Y., Deng, C., Xu, H., Xie, Z., & Ruan, C. (2024). DeepSeek-VL: Towards Real-World Vision-Language Understanding. *arXiv preprint arXiv:2403.05525*.
14. Yin, X., Zhu, Y., & Hu, J. (2021). A comprehensive survey of privacy-preserving federated learning: A taxonomy, review, and future directions. *ACM Computing Surveys*, 54(6), 1-36. <https://doi.org/10.1145/3460427>
15. Ioannidis, J. P. A. (2005). Why most published research findings are false. *PLoS Medicine*, 2(8), e124. <https://doi.org/10.1371/journal.pmed.0020124>
16. Munafò, M. R., Nosek, B. A., Bishop, D. V. M., Button, K. S., Chambers, C. D., Percie du Sert, N., Simonsohn, U., Wagenmakers, E. J., Ware, J. J., & Ioannidis, J.

P. A. (2017). A manifesto for reproducible science. *Nature Human Behaviour*, 1(1), 0021. <https://doi.org/10.1038/s41562-016-0021>

17. Jain, G., Hegde, N., Kusupati, A., Nagrani, A., Buch, S., Jain, P., Arnab, A., & Paul, S. (2024). Mixture of Nested Experts: Adaptive Processing of Visual Tokens. arXiv preprint arXiv:2407.19985.
18. Zhang, Z., Pham, P., Zhao, W., Wan, K., Li, Y.-J., Zhou, J., Miranda, D., Kale, A., & Xu, C. (2024). Treat Visual Tokens as Text? But Your MLLM Only Needs Fewer Efforts to See. arXiv preprint arXiv:2410.05243.
19. Li, K. Y., Goyal, S., Dias Semedo, J., & Kolter, J. Z. (2024). Inference Optimal VLMs Need Fewer Visual Tokens and More Parameters. arXiv preprint arXiv:2411.03312.
20. Wang, Y., Liu, C., Qu, Y., Cao, H., Jiang, D., & Xu, L. (2024). Break the Visual Perception: Adversarial Attacks Targeting Encoded Visual Tokens of Large Vision-Language Models. arXiv preprint arXiv:2411.03312.

Figures: 11 (1: PHI bbox to patch pipeline; 2: Coordinate mapping; 3: DeepSeek-OCR architecture with hook points; 4: Compression leakage schematic; 5: Masking variant convergence; 6: PHI masking success by type; 7: Hybrid defense-in-depth flow; 8: Hybrid swimlane PHI coverage; 9: Failure modes and mitigations; 10: Future work roadmap; 11: Spatial coverage vs PHI reduction)

Tables: 2 (Table 1: Masking strategies; Table 2: Hybrid pipeline)

Code Availability: Implementation (failed experiment) will be archived on GitHub; URL to be added.

Data Availability: Synthetic data can be regenerated using Synthea; scripts available in-repo.

Competing Interests: The authors declare no competing interests.

Funding: None.